Effect of *de novo* transcriptome assembly on transcript quantification

Ping-Han Hsieh[1], Yen-Jen Oyang[1, 2] and Chien-Yu Chen[3, 4 *]

[1] Graduate Institute of Biomedical Electronics and Bioinformatics, National Taiwan University, Taipei 10617, Taiwan. [2] Department of Computer Science and Information Engineering, National Taiwan University, Taipei 10617, Taiwan. [3] Department of Bio-Industrial Mechatronics Engineering, National Taiwan University, Taipei 10617, Taiwan. [4] Genome and Systems Biology Program, National Taiwan University and Academia sinica, Taipei 10617, Taiwan.

[*] Corresponding authors

Chien-Yu Chen
Department of Bio-Industrial Mechatronics Engineering, National Taiwan University, Taipei 10617, Taiwan.
Phone: +886-2-3366-5334, E-mail: chienyuchen@ntu.edu.tw

E-mail addresses

Ping-Han Hsieh: dn070017@gmail.com
Yen-Jen Oyang: yjoyang@csie.ntu.edu.tw
Chien-Yu Chen: chienyuchen@ntu.edu.tw

Abstract

Background: Correct quantification of transcript expression is essential to understand the functional products of the genome in different physiological conditions and developmental stages. Recently, the development of high-throughput RNA sequencing (RNA-Seq) allows the researchers to perform transcriptome analysis for the organisms without the reference genome and transcriptome. For such projects, *de novo* transcriptome assembly must be carried out prior to quantification. However, a large number of erroneous contigs produced by the assemblers might result in unreliable estimation on the abundance of transcripts. In this regard, this study comprehensively investigates how assembly quality affects the performance of quantification for RNA-Seq analysis based on *de novo* transcriptome assembly.

Results: Several important factors that might seriously affect the accuracy of the RNA-Seq analysis were thoroughly discussed. First, we found that the assemblers perform comparatively well for the transcriptomes with lower biological complexity. Second, we examined the over-extended and incomplete contigs, and then demonstrated that assembly completeness has a strong impact on the estimation of contig abundance. Lastly, we investigated the behavior of the quantifiers with respect to sequence ambiguity which might be originally present in the transcriptome or accidentally produced by assemblers. The results suggest that the quantifiers

often over-estimate the expression of family-collapse contigs and under-estimate the expression of duplicated contigs. While it remained challenging to detect the inaccurate abundance estimation on family-collapse contigs, on the contrary, we observed that the situation of under-estimation on duplicated contigs can be warned through analyzing the read distribution of the contigs in the same connected component.

Conclusions: In summary, we explicated the behavior of quantifiers when erroneous contigs are present and we outlined the potential problems that the assemblers might cause for the downstream analysis of RNA-Seq. We anticipate the analytic results conducted in this study provides valuable insights for future development of transcriptome assembly and quantification.

Background

Quantification and comparison of transcript expression are essential to understanding the role of RNA in different physiological conditions or developmental stages. Such experiments and analyses are widely used in the studies of molecular biology. Over the past decades, several biological technologies have been developed to quantify the abundance of transcripts, such as expression microarray [1] and high-throughput RNA sequencing (RNA-Seq) [2]. For organisms with sufficient genomic information, the design of microarray provides a high throughput and cost-effective solution to examine transcript expression. On the other hand, RNA-Seq is superior in delivering lower background signals and larger dynamic ranges [3]. Despite the fact that many genome sequencing projects have been carried out, such as Genome10K [4], 5000 arthropod genomes initiative (i5K) [5] and Bird10K [6], whole genome studies are still demanding efforts for many research groups because of the immense cost and time-consuming process. For non-model organisms, the expression microarray needs to rely on cross-species hybridization [7]. On the contrary, RNA-Seq is more suitable owing to its capability of detecting novel transcripts without additional genomic information [3].

When the reference genome and transcriptome are not available, RNA-Seq reads are first used to reconstruct the transcriptome [8, 9]. Nowadays, many programs have been developed

66 for *de novo* transcriptome assembly, such as Oases [10], rnaSPAdes [11], SOAPdenovo-Trans
67 [12], Trans-ABySS [13] and Trinity [14]. After transcriptome sequences are reconstructed,
68 quantification methods including BitSeq [15], Kallisto [16], RSEM [17] and Salmon [18] can
69 be applied. These methods are able to inference the abundance of expression without the need
70 of genomic sequences, using the number of RNA-Seq reads that overlap with the assembled
71 contigs [9]. Nevertheless, quantification is much more challenging without reliable reference
72 sequences because of the erroneous contigs produced by the assemblers, which often result
73 from sequencing errors, insufficient sequencing depth and biological variability [19]. To
74 address these problems, a great number of comparative studies have been published recently.
75 While many studies evaluated transcriptome assembly [19-21] or quantification [22, 23]
76 programs independently, few have discussed how transcriptome assembly influences the
77 downstream quantification analysis. In 2013, Vijay, N., *et al*. performed an *in silico* assessment
78 of RNA-Seq experiments. That study examined the impact of various aspects of sequencing
79 reads on transcriptome assembly and differentially expressed genes (DEG) analysis [7], but the
80 effect of redundant contigs and multiple-mapping reads on quantification was not well
81 discussed. Another study conducted by Wang, S. and M. Gribskov evaluated the quality of
82 assembled contigs and their effects on DEG analysis [24]. However, their study mainly focused

83 on the evaluation of entire workflow from assembly, quantification, to DEG analysis, which
84 makes it obscure to unravel how the erroneous contigs affect the authenticity of downstream
85 analysis.

86 This study aims comprehensively discussing the effect of biological complexity on
87 transcriptome assembly, as well as the influence of incomplete and over-extended contigs on
88 quantification We used both *in silico* simulated and authentic RNA-Seq data from three species
89 (yeast, dog, and mouse) to examine the effect of biological complexity on *de novo* transcriptome
90 assembly. Three state-of-the-art assemblers, namely rnaSPAdes, Trinity and Trans-ABySS,
91 were evaluated under different biological complexities based on TransRate [19] scores, which
92 were previously proposed to assess the quality of *de novo* transcriptome assemblies using the
93 alignments of sequencing reads to the assembled sequences. After *de novo* assembly, the
94 reference transcripts were assigned to assembled contigs according to the BLASTn [25]
95 alignments. Each transcript-contig alignment was then categorized based on accuracy, recovery
96 and sequence ambiguity. Subsequently, we thoroughly examined the impact of erroneous
97 contigs on the quantifiers Kallisto, RSEM and Salmon. By exploring the interplay between each
98 stage in RNA-Seq analysis workflow, this study provides valuable insights into conducting
99 RNA-Seq analysis and we anticipate these discoveries would be useful in the future

100 development of assembly or quantification algorithms.

101

102 ## Materials and Methods

103 **Datasets**

104 Three experimental and three simulated RNA-Seq datasets were used in this study. Both
105 experimental and simulated data included three species: yeast (*Saccharomyces cerevisiae*), dog
106 (*Canis lupus familiaris*) and mouse (*Mus musculus*). The experimental datasets were collected
107 from the Sequence Read Archive (SRA). The yeast dataset (SRR453566) was from the study
108 of Nookaew *et al.* [26], comprising 5.5 million non-stranded paired-end reads cultivated under
109 the batch condition. The dog dataset (SRR882109) was produced by Liu, *et al.* [27], comprising
110 20.8 million non-stranded paired-end reads sampled from normal mammary gland tissues of
111 domestic dogs. Finally, the mouse dataset (SRR203276) was collected from the study of
112 Grabherr, *et al* [14], containing 43.4 million stranded paired-end reads extracted from dendritic
113 cells. For the simulated datasets, Flux Simulator (ver. 1.2.1) [28] was adopted to synthesize
114 RNA reads for yeast, dog and mouse, respectively, based on the genomic sequences and
115 annotations from the Ensembl database [29]. To facilitate the analysis, only the transcripts
116 annotated as messenger RNA (mRNA) and with over 500 nucleotides in length were extracted.

117 The parameters used for the simulation are shown in Additional File 1: Table S1. In total, 81.7
118 million non-stranded paired-end reads were generated for the assembly and quantification
119 analysis. The quality of both experimental and simulated datasets was examined using FastQC
120 (ver. 0.11.5) [30] and the low-quality subsequences of the reads were trimmed using
121 Trimmomatic (ver. 0.36) [31] with parameters *SLIDINGWINDOW:4:20 MINLEN:30*. The
122 resultant RNA reads that were unable to maintain the paired relation were discarded. The
123 detailed information of the processed RNA reads is provided in Additional File 1: Table S2
124 (The mean and standard deviation of the insert sizes were estimated based on the alignments
125 produced by Burrows-Wheeler Aligner [32]).
126
127 **Expression Metrics**
128 In order to evaluate the performance of transcript quantification, the ground truth of expression
129 abundance for each transcript must be first determined. For simulated datasets, the numbers of
130 the generated RNA reads for each transcript was recorded during the simulation process. Since
131 transcriptome assemblers sometimes generate duplicated, incomplete or over-extended contigs,
132 the metrics we use for quantifying expression must consider the normalization with respect to
133 both sequence length and the number of total nucleotides. In this regard, the number of

134 generated RNA reads was transformed into a simplified version of Transcripts per Million

135 (TPM) [33] using the following equation:

136 $$\text{Ground Truth TPM}_i = \frac{f_i/l_i}{\sum_{k=1}^{n} f_k/l_k} \times 10^6,$$

137 where n is the total number of transcripts, f_i is the number of RNA reads generated from

138 transcript i and l_i is the effective length [34] of transcript i. In contrast, because the ground

139 truth abundance for each RNA molecule is unknown for experimental datasets, we calculated

140 the average TPM inferred by Kallisto (ver. 0.43.0), RSEM (ver. 1.2.31) (default parameters)

141 and Salmon (ver. 0.8.2) for the reference transcript as the ground truth expression when

142 evaluating the abundance of an assembled contig. Although the estimated expression might not

143 perfectly reflect the real number of RNA molecules in a biological sample, it still provides

144 valuable information when comparing the performance of quantification before and after *de*

145 *novo* transcriptome assembly.

146

147 ***de novo* Transcriptome Assembly and Quantification**

148 The processed RNA-Seq reads were assembled into contigs using the following three programs:

149 (1) rnaSPAdes (ver. 3.11.1), (2) Trans-ABySS (ver. 1.5.5) along with ABySS (ver. 1.5.2) [35]

150 and (3) Trinity (ver. 2.4.0) with default parameters. To minimize the effect of fragmented

151 contigs, only the contigs with over 500 nucleotides in length were kept for the quantification
152 analysis. The assemblies were evaluated based on the length of contigs, the number of
153 recovered transcripts, the number of erroneous contigs and the evaluation scores provided by
154 TransRate. The TransRate scores that we used in this study are the *score of bases covered*, *score*
155 *of good mapping*, *score of not segmented* and *overall score*. The score of bases covered
156 represents the proportion of nucleotide bases in a contig that are covered by reads. The score of
157 good mapping represents the proportion of read pairs of which both reads are aligned in the
158 correct orientation on a single contig. The score of not segmented represents the proportion of
159 contigs that might be a chimera of multiple transcripts. Subsequently, the expression abundance
160 for each contig was estimated using one alignment-based and two alignment-free quantifiers,
161 namely (1) Bowtie2 (ver. 2.3.0) [36] (*--dpad 0 --gbar 99999999 --mp 1,1 --np 1 --score-min*
162 *L,0,-0,1 -k 200 --sensitive --no-mixed --no-discordant*) followed by RSEM (ver. 1.2.31) (default
163 parameter*s*); (2) Kallisto (ver. 0.43.0) (indexing with *-k 31* and quantifying with default
164 parameters); and (3) Salmon (ver. 0.8.2) (indexing with *-k 31* and quantifying with default
165 parameters).
166
167 **Transcript Assignment**

168 For the purpose of comparing the estimated abundance of contigs with the ground truth
169 expression from the corresponding transcripts, we assigned the reference transcripts to
170 assembled contigs based on BLASTn (2.5.0+) [25] alignments. Here, only the high scoring
171 pairs (HSPs) with identity over 70% and E-value smaller than 1E−5 were considered. We
172 integrated the remained HSPs onto the coordinates of both transcript and contig to obtain the
173 global alignment. Similar to a previous study [7], we calculated the *recovery* and *accuracy* for
174 each global alignment, which refer to the proportion of matched nucleotides on the transcript
175 and the proportion of correctly matched nucleotides on the contig respectively (Additional File
176 2: Fig. S1). Furthermore, we defined the overall *alignment score* as $\sqrt{recovery \times accuracy}$. A
177 transcript is assigned to a contig if either *accuracy* or *recovery* of the global alignment between
178 them is above 90%. In this manner, we were able to identify all the corresponding transcripts
179 for each contig. Note that it is possible that a contig can be associated with multiple transcripts,
180 and a transcript can assign to multiple contigs as well. We considered multiple assignments here
181 in order to understand the impact of redundant sequences on the quantification. Once the
182 transcripts have been assigned to the contigs, we used the following equation to calculate the
183 relative error of expression, in order to evaluate the quality of transcript quantification for each
184 transcript-contig pair:

185 $$\text{Relative Error}_{(i,\,j)} = \frac{TPM_i^{est} - TPM_j^{g.t}}{TPM_i^{est} + TPM_j^{g.t}} \times 100\%,$$

186 where the TPM_i^{est} is the expression estimated by quantifiers for $contig_i$, and the $TPM_j^{g.t}$ is the

187 ground truth expression for $transcript_j$ given ($contig_i$, $transcript_j$) is a valid global alignment

188 (either *accuracy* or *recovery* of the global alignment between them is above 90%).

189

190 **Sequence Ambiguity**

191 To determine the origin of the RNA-Seq reads that can be mapped to multiple transcripts is an

192 important issue for the development of quantification algorithms. In this regard, it is of interest

193 to understand the impact of sequence ambiguity on transcript quantification. We performed

194 pairwise sequence alignment on both transcripts and contigs using BLASTn, respectively. Here,

195 only the HSPs with identity over 70% and E-value smaller than 1E−5 were considered as

196 potential ambiguity. In addition, to better explicate the relation between sequences that share

197 similar subsequences, we build a connected component graph, where two sequences were

198 grouped into the same connected component if the proportion of identical nucleotides between

199 them is over 90% of the either sequence (Fig. 1). The size of a connected component is defined

200 as the number of sequence members inside. We call the sequences in a connected component

201 containing only one sequence as *unique sequence*. Furthermore, we used the read proportion of

202 estimated abundance (RPEA) to investigate the behavior of quantifier while ambiguous

203 sequences are presented. Given n contigs $c_1, c_2, c_3 \ldots c_n$ in the same connected component C,

204 the RPEA score for each contig is defined as follow:

205 $$\text{RPEA}_i = \frac{\text{Allocated Read Count for } c_i}{\sum_{j=1}^{n} \text{Allocated Read Count for } c_j}.$$

206 If the highest RPEA in the connected component is close to 1, it suggests that the quantifier

207 allocates all the reads in the connected component to one specific contig. In contrast, if the

208 highest RPEA in the connected component is close to $1/n$, then it suggests that the quantifier

209 tends to allocate the reads evenly in the connected component.

210

211 **Contig Categories**

212 The assembled contigs are categorized into five particular categories in this study: (1) *full-*

213 *length*, (2) *incompleteness*, (3) *over-extension*, (4) *family-collapse* and (5) *duplication* (Fig. 2).

214 The analysis of the first three categories were not affected by the factor of sequence ambiguity,

215 allowing us to investigate the impact of assembly completeness on quantification independently.

216 Given the length of contig l_c and the length of the corresponding transcript l_t, the

217 completeness of a contig was examined through the difference in length:

218 $$\text{Difference in Length}_{(c,\, t)} = \frac{l_c - l_t}{l_c + l_t} \times 100\%.$$

219 In contrast, *family-collapse*, *duplication* and *multiple-alignment* focused on the contigs that
220 completely recovered the transcripts (*recovery* $\geq$ 90) but considered the influence of sequence
221 ambiguity. To be more specific, *family-collapse* represents contigs which are assigned with
222 multiple transcripts and *duplication* stands for the multiple contigs assigned by a single
223 transcript. By examining these contigs, the problems caused by the assemblers that fail to
224 distinguish similar transcripts from each other or generate a large number of redundant contigs
225 are investigated. The detailed definitions for contig categories are provided in Additional File
226 1: Table S3.
227

228 ## Results

229 ### *de novo* Transcriptome Assembly

230 Based on pairwise BLASTn, yeast has the simplest transcriptome, with 94.11% of the
231 transcripts sharing no similar subsequences with others. We call these sequences unique
232 transcripts in the transcriptome. On the other hand, 66.29% of the dog transcripts are unique,
233 while only 28.45% of the mouse transcripts are unique (Additional File 1: Table S4). First, we
234 performed transcriptome assembly on the RNA reads of the three species with different
235 biological complexities. We adopted three assemblers, rnaSPAdes, Trans-ABySS and Trinity,

236 to construct contigs for both experimental and simulated RNA-Seq reads. Next, we built
237 connected components for the assembled contigs. The statistics of sequence length and
238 sequence ambiguity for the assembled contigs are shown in Additional File 1: Table S5, while
239 the numbers of contigs that were categorized in each contig category are shown in Additional
240 File 1: Table S6. The proportion of recovered transcripts (*recovery* $\geq$ 90) and accurate contigs
241 (*accuracy* $\geq$ 90) is shown in Additional File 2: Fig. S2, and finally, the TransRate scores for
242 each assembly are shown in Additional File 2: Fig. S3.

243 In general, rnaSPAdes constructed the least amount of contigs with the highest overall
244 TransRate score for most of the datasets (5 among 6 datasets). As shown in Additional File 1:
245 Table S5, rnaSPAdes also delivered the lowest average size of the connected components across
246 species, suggesting that the contigs generated by rnaSPAdes are less redundant when compared
247 to those from the other two assemblers. Trinity outperformed other assemblers in terms of N50
248 and the proportion of the recovered transcripts in all the simulated datasets. Despite the fact that
249 Trinity generated longer contigs, the overall TransRate scores and the proportions of accurate
250 contigs from Trinity assembly are marginally lower. Trans-ABySS constructed the contigs with
251 comparatively high accuracy, with 66.37% of the contigs aligned with at least one transcript
252 that show accuracy higher than 0.90. Nonetheless, Trans-ABySS constructed smaller numbers

253 of unique and long contigs relatively. In other words, Trans-ABySS generated shorter contigs
254 with more redundancy. The summary of the assemblies also demonstrates that the proportion
255 of recovered transcripts are significantly higher in the datasets of yeast than that of dog or
256 mouse. With higher complexity, it appears to become more difficult for the assemblers to
257 properly reconstruct the transcriptome. For the estimated abundance of assembled contigs, the
258 estimation made by quantifiers RSEM, Kallisto and Salmon shows considerably high
259 consistency (Additional File 2: Fig. S4), with both Pearson's and Spearman's correlation
260 coefficients higher than 0.95 between any of the two quantifiers.
261
262 **Impact of Assembly Completeness**
263 In this study, the influence of *de novo* transcriptome assembly on expression quantification is
264 mainly discussed with respect to two major issues: assembly completeness and sequence
265 ambiguity. We would like to primarily look into the impact of assembly completeness on
266 quantification in this section. In order to reduce the possible effect of sequence ambiguity
267 generated by the assemblers, only the unique contigs (contigs in a connected component
268 containing only itself) that are assigned with a single transcript were examined here. The unique
269 contigs were further categorized into *full-length*, *incompleteness* and *over-extension* (see

270 Methods for detailed definitions). The reliability of quantification was examined based on the
271 relative error for contigs with different extent of assembly completeness (Fig. 3).
272 In summary, full-length contigs show the lowest relative error of quantification, with the
273 medians of error smaller than ±10%. The scatter plots and correlation coefficients also suggest
274 that the estimated abundance of full-length contigs is highly reliable, with Pearson's and
275 Spearman's correlation coefficient between the estimated and ground truth abundance both
276 larger than 0.97 in all the datasets (Fig. 4, Fig. 5). The incomplete contigs yield slight over-
277 estimation on the expression abundance. Overall, the quantification errors gradually increased
278 as the assembly completeness decreased. This phenomenon can be observed more obviously
279 on the dog and mouse datasets. When compared with the full-length contigs, the correlation
280 coefficients are comparatively lower, ranging from 0.70 to 0.94 (Fig. 4, Fig. 5). Lastly, for the
281 category of over-extended contigs, the quantifiers underestimated the expression abundance
282 and the correlation coefficients slightly dropped (Fig. 4, Fig. 5). Nevertheless, the number of
283 over-extended contigs is much fewer than those of other categories (Additional File 1: Table
284 S6), which indicates that the assemblers did not overly extend the assembled contigs in most of
285 the cases. In other words, only a limited number of contigs in the quantification will be affected
286 in the practical RNA-Seq analysis. Although the TPM metrics has already been normalized for

287 sequence length and total nucleotides, researchers might still need to be aware of the length
288 bias caused by incomplete or over-extended contigs while using TPM as the metrics to estimate
289 the expression of contigs.
290
291 **Impact of Sequence Ambiguity**
292 In this section, the impact of sequence ambiguity on quantification was thoroughly discussed.
293 Similarly, to reduce the compound effect from assembly completeness, only the accurately
294 assembled contigs (*accuracy* $\geq$ 90) were examined here. In the first part of this sub-section,
295 we looked through the reliability of quantification when the assemblers report only one contig
296 for many similar transcripts, denoted as *family-collapse*. In the second part, we examined the
297 impact of contigs with similar sequence content which are assigned with the same transcript,
298 denoted as *duplication* (see Methods for detailed definition). By using these contigs, we
299 examined the behavior of the quantification algorithms while sequence ambiguity is present in
300 the assembly.
301 For the contigs categorized as family-collapse, it is much more difficult to analyze the
302 accuracy of quantification because of multiple transcripts being assigned to a contig. Based on
303 our observation, there are in average 2 to 3.16 transcripts being assigned to a family-collapse

304 contig across the six datasets. Since there is only one contig that were assigned by multiple
305 transcripts, we would like to find out of which transcript expression delivers the estimated
306 abundance of the contig actually reflects. To our surprise, the estimated abundance is closer to
307 the transcript with the highest expression rather than the one with highest alignment score (Fig.
308 6, Additional File 2: Fig. S5).

309 In contrast with family-collapse, duplication represents the redundant contigs which are
310 clustered into the same connected component and are assigned with a single transcript. Here,
311 we use the maximum estimated abundance in the connected component to investigate the
312 behavior of quantifiers (see Methods for detailed definition). We observed that quantification
313 algorithms tend to allocate most of the RNA reads to a single contig within the connected
314 component in most of the cases (15 out of 18 of the datasets show that over 50% of the
315 connected component has one contig with the proportion of estimated abundance over 75%)
316 (Additional File 2: Fig. S6). Furthermore, we would like to understand which estimated
317 abundance of the contig in the connected component can accurately reflect the expression of
318 corresponding transcript. Here, we used three approach to select the estimated abundance of
319 the contig in the connected component: (1) the contigs with the highest alignment score, (2) the
320 contigs that are allocated with the most RNA reads and (3) the total expression of connected

321 component of the contigs. Consequently, we found that the estimated abundance of contigs that
322 were allocated with the most amount of RNA reads in the connected component show
323 significantly low quantification error with the transcript expression. However, in the cases when
324 the quantifiers distribute the RNA reads evenly to the duplicated contigs, the ground truth
325 expression for the transcripts cannot be accurately represented by the estimated abundance of
326 contigs. (Fig. 7). To address this problem, it is advisable to use the total expression of the
327 connected component for duplicated contigs to measure the expression of corresponding
328 transcripts.
329
330 **Discussions**
331 **Component-level Quantification**
332 Based on the observation discussed in the previous section, we first discovered that once the
333 assemblers failed to distinguish the RNA reads generated from similar transcripts and reported
334 one single contig, the estimated abundance of family-collapse contigs often reflect the
335 expression of the transcripts generating the most amount of RNA reads. In contrast, to estimate
336 the expression of transcripts corresponding to the duplicated contigs, researchers might need to
337 use to abundance of the contigs that are allocated with the majority of the RNA-reads (highest
338 RPEA score) in order to get accurate estimation. Nevertheless, these conclusions are drawn

339 from the strictly defined scenario. In most of the practical RNA-Seq analysis, the information
340 of the transcriptome sequence is not available for non-model organisms. Therefore, it is
341 essential to understand which approach is the best suited to select the contigs and the
342 corresponding transcripts with the closest estimation on abundance. Here, we looked through
343 all the valid assignment of transcripts for each contig and we demonstrated four different
344 methods: (1) selecting the transcripts with the highest alignment score for each contig, followed
345 by selecting the contig with the highest alignment score for each transcript, (2) selecting the
346 transcripts with the highest alignment score for each contig, followed by selecting the contig
347 with the highest RPEA score in the connected component, (3) selecting the transcripts with the
348 highest expression in the connected component, followed by selecting the contig with the
349 highest alignment score for each transcript, and (4) selecting the transcripts with the highest
350 expression in the connected component, followed by selecting the contig with the highest RPEA
351 score in the connected component. As a result, it seems to be more appropriate to use the
352 estimated abundance of contigs with the highest RPEA score in the connected component to
353 reflect the expression of transcripts (Fig. 8). Despite the fact that this strategy forgo the concept
354 of quantification for individual transcripts, many advantages emerge such as higher accuracy
355 on the quantification, reliable read inference, robust statistical performance and clear

356 interpretation of the data [37]. More importantly, this strategy does not have to deal with the
357 thorny problem resulting from multiple transcript assignment in contig annotation.
358
359 **The Selection of Programs**
360 We argue that the difficulties discussed in this research emerge mainly because the goals for
361 each step of the analysis is not specifically designed to suit *de novo* RNA-Seq analysis. Most
362 of the assemblers are optimized to reconstruct the whole transcriptome, which sometimes leads
363 to many false predictions on SNPs or isoforms. These artificial or incorrect contigs thereafter
364 deteriorate the accuracy of quantifiers because most of the quantification algorithms infer the
365 expression based on the overlapping relation between RNA-Seq reads and the given sequences
366 (transcripts or contigs). Furthermore, the annotation step often utilizes programs that excel in
367 sequence alignment without considering the abundance of expression. This observation
368 demonstrates that the selection of the programs has a strong impact on the *de novo* RNA-Seq
369 analysis. For instance, to minimize the effect of assembly completeness on quantification,
370 assemblers that construct the sequences with appropriate length are preferable. On the other
371 hand, to reduce the problem in contig annotation resulting from sequence ambiguity, the
372 assemblers that report less false prediction for SNPs or isoforms are better choices. The

373 performance for the quantifiers we analyzed throughout this study demonstrates high
374 consistency in terms of accuracy of quantification. Therefore, we recommended to use the
375 alignment independent quantifiers such as Kallisto and Salmon for significantly lower
376 computational time [16, 18]. The selection of programs for contig annotation is relatively
377 irrelevant because the bottleneck mainly lies in the insufficient transcript information. Since
378 there are no reference transcripts available in the practical *de novo* RNA-Seq analysis, most of
379 the research utilizes the protein sequences from proximate species with small genetic changes
380 because of comparatively higher conservation in protein sequences. However, to align the
381 contigs with proteins of other species might reduce the precision and accuracy of sequence
382 alignment, which makes it more difficult to find the correct annotation for the assembled contigs.
383

384 **Other Important Factors in RNA-Seq Analysis**

385 Although we mainly discussed the impact of assembly completeness and sequence ambiguity
386 on quantification and annotation throughout this study, there are many other factors that might
387 as well result in unreliable experimental results in the practical *de novo* RNA-Seq analysis. For
388 instance, the read length or the fragment size directly determine the maximum length of the
389 nucleotides that overlap with the reference sequences for each read pair. Therefore, the number

390 of RNA-Seq reads that can be aligned to multiple origins of the transcripts reduces when longer
391 reads are adopted, which mitigates the problem of sequence ambiguity on the inference of the
392 origin of the reads [33, 34]. The strand specificity provides the information for the strand of the
393 RNA-Seq reads, which improves the precision of sequence alignment and quantification [38].
394 Last but not least, the sequence-specific and positional bias derived from library construction
395 might lead to RNA-Seq reads that over- or under-represent the number of transcripts in the
396 molecules In this regard, it is important to model the fragment bias in the process of
397 quantification [39]. However, considering all the combined effects of the factors mentioned
398 above will significantly increases the complexity of this research. Therefore, we generated non-
399 stranded RNA-Seq with uniform read length, and the fragment bias for the reads were excluded.
400 Moreover, the start coordinates of the RNA-Seq reads uniformly distributed. By this means, we
401 excluded the potential impact of these factors and focused only on the effect of assembly
402 completeness and sequence ambiguity. But the importance of these factors should not be
403 ignored in the practical *de novo* RNA-Seq analysis.
404
405 **Sequencing Technologies**

406 In this section, we briefly highlight two sequencing technologies that provide another new
407 perspective and mitigate the problems in RNA-Seq analysis: single-cell RNA sequencing
408 (scRNA-Seq) and long-read RNA sequencing. By isolating individual cell prior to sequencing,
409 scRNA-Seq technology allows the researchers to extract mRNA from a single cell. The
410 development of scRNA-Seq allows the researchers to identify uncharacterized cell types, to
411 observe the stochastic nature of gene expression, and to compare the expression profiles for the
412 individual cells within the population [9, 40]. Nevertheless, the number of reads generated using
413 scRNA-Seq is relatively small since only a small number of mRNA molecules are expressed in
414 a single cell. This drawback makes it difficult to reconstruct the transcriptome for each cell
415 [40]. Moreover, assembly algorithms that take the advantages of unique molecular identifiers
416 (UMIs) for each read are still in demand. In the *de novo* RNA-Seq analysis, it is advisable to
417 aggregate the scRNA-Seq from all cells as the bulk RNA-Seq reads to reconstruct the
418 transcriptome and subsequently estimate the abundance of each cell subsequently. The
419 restriction makes the exploitation of scRNA-Seq mainly limit to species with highly-curated
420 transcript sequences available.

421 Another technology that developed with increasing interests recently is long-read RNA
422 sequencing. Unlike next-generation RNA-Seq technology, long-read RNA sequencing

423 generates a single read for each mRNA molecule in real-time, which results in considerably
424 longer RNA-Seq data that allows the full-length reconstruction for transcripts without the need
425 of assembly [9]. Although the demanding cost for sequencing in higher coverage makes it hard
426 to be considered for quantification at this moment, this technology still provides an
427 extraordinary breakthrough for identifying the transcriptome in non-model organisms [41]. If
428 the research expenditure is sufficient, we recommend combining the long-read technology with
429 scRNA-Seq reads for the identification and quantification of the novel transcriptome
430 respectively.
431

432 **Conclusion**

433 While most of the related studies focused on optimizing the quantification or assembly
434 algorithms independently, few studies have discussed how the erroneous contigs generated by
435 the assemblers affect the downstream analysis of RNA-Seq. In this study, we comprehensively
436 examined the impact of biological complexity, assembly completeness and sequence ambiguity.
437 We comparatively evaluated the performance of rnaSPAdes, Trans-ABySS and Trinity for *de*
438 *novo* transcriptome assembly under three transcriptomes with different complexities. All of the
439 selected assemblers showed a lower proportion of the fully-reconstructed transcripts as the

440 complexity of transcriptome increases. In general, rnaSPAdes constructed the least number of
441 contigs with the highest TransRate score, Trinity produced the longer contigs, and Trans-
442 ABySS generated the contigs with the higher accuracy. As for quantification, we measured the
443 reliability of RSEM, Kallisto and Salmon. The estimation made by three algorithms shows
444 marginal differences. For each erroneous contig, the incomplete or over-extended contigs lead
445 to unreliable estimation of the abundance of contigs. Moreover, we have found that if the
446 redundant contigs are present in the assembly, the quantifiers tended to allocate the RNA-Seq
447 reads to one of the duplicated contig. However, in rare cases, the quantifiers distributed the
448 reads evenly to the contigs that share similar sequence content. On the contrary, the quantifiers
449 tended to over-estimate the contigs that were assigned with multiple transcripts since the
450 assemblers failed to distinguish the difference of these transcripts and reported only a single
451 contig. To circumvent these issues, it is advisable to estimate the abundance on gene-level rather
452 than for individual transcripts using tools such as Corset. By exploring how these factors
453 deteriorate the reliability of *de novo* RNA-Seq analysis, we provided valuable insights for the
454 interplay between transcriptome assembly, quantification and sequence annotation. We
455 anticipated these discoveries will be useful in the future development of assembly or
456 quantification programs.

457

Declarations

Ethics approval and consent to participate

Not applicable.

Consent for publication

Not applicable.

Availability of data and material

The analysis pipelines used in this study are available and can be downloaded from GitHub repository: https://github.com/dn070017/QuantEval. The RNA reads supporting the results of this article are available in the NCBI Short Read Archive, with the accession numbers SRR453566 (yeast) and SRR882109 (dog), SRR203276 (mouse).

Competing interests

The authors declare that they have no competing interests.

Funding

The authors would like to thank Ministry of Science and Technology (MOST), R. O. C., for the financial support under the contract: MOST 105-2627-M-002-027.

Authors' contributions

Ping-Han Hsieh performed the analysis and wrote the manuscript. Chien-Yu Chen and Yen-Jen Oyang commented on the draft and revised the manuscript. All authors read and approved the final manuscript.

Acknowledgements

We wish to thank Yu-Chuan Chang and Mei-Ju May Chen for discussion on the analysis of quantification, Dr. Mong-Hsun Tsai for the comments on the analysis of RNA-Seq technology and Dr. Li-Yu Liu for the advices on statistical inference.

488 ## Reference

489 1. Schena M, Shalon D, Davis RW, Brown PO: **Quantitative monitoring of gene**
490 **expression patterns with a complementary DNA microarray**. *Science* 1995,
491 **270**(5235):467-470.
492 2. Mortazavi A, Williams BA, McCue K, Schaeffer L, Wold B: **Mapping and quantifying**
493 **mammalian transcriptomes by RNA-Seq**. *Nat Methods* 2008, **5**(7):621-628.
494 3. Wang Z, Gerstein M, Snyder M: **RNA-Seq: a revolutionary tool for transcriptomics**.
495 *Nat Rev Genet* 2009, **10**(1):57-63.
496 4. Genome KCoS: **Genome 10K: a proposal to obtain whole-genome sequence for**
497 **10,000 vertebrate species**. *J Hered* 2009, **100**(6):659-674.
498 5. i KC: **The i5K Initiative: advancing arthropod genomics for knowledge, human**
499 **health, agriculture, and the environment**. *J Hered* 2013, **104**(5):595-600.
500 6. Zhang G, Rahbek C, Graves GR, Lei F, Jarvis ED, Gilbert MT: **Genomics: Bird**
501 **sequencing project takes off**. *Nature* 2015, **522**(7554):34.
502 7. Vijay N, Poelstra JW, Kunstner A, Wolf JB: **Challenges and strategies in**
503 **transcriptome assembly and differential gene expression quantification. A**
504 **comprehensive in silico assessment of RNA-seq experiments**. *Mol Ecol* 2013,
505 **22**(3):620-634.
506 8. Martin JA, Wang Z: **Next-generation transcriptome assembly**. *Nat Rev Genet* 2011,
507 **12**(10):671-682.
508 9. Conesa A, Madrigal P, Tarazona S, Gomez-Cabrero D, Cervera A, McPherson A,
509 Szczesniak MW, Gaffney DJ, Elo LL, Zhang X *et al*: **A survey of best practices for**
510 **RNA-seq data analysis**. *Genome Biol* 2016, **17**:13.
511 10. Schulz MH, Zerbino DR, Vingron M, Birney E: **Oases: robust de novo RNA-seq**
512 **assembly across the dynamic range of expression levels**. *Bioinformatics* 2012,
513 **28**(8):1086-1092.
514 11. Bankevich A, Nurk S, Antipov D, Gurevich AA, Dvorkin M, Kulikov AS, Lesin VM,
515 Nikolenko SI, Pham S, Prjibelski AD *et al*: **SPAdes: a new genome assembly**
516 **algorithm and its applications to single-cell sequencing**. *J Comput Biol* 2012,
517 **19**(5):455-477.
518 12. Xie Y, Wu G, Tang J, Luo R, Patterson J, Liu S, Huang W, He G, Gu S, Li S *et al*:
519 **SOAPdenovo-Trans: de novo transcriptome assembly with short RNA-Seq reads**.
520 *Bioinformatics* 2014, **30**(12):1660-1666.

521 13. Robertson G, Schein J, Chiu R, Corbett R, Field M, Jackman SD, Mungall K, Lee S,
522 Okada HM, Qian JQ *et al*: **De novo assembly and analysis of RNA-seq data**. *Nat*
523 *Methods* 2010, **7**(11):909-912.
524 14. Grabherr MG, Haas BJ, Yassour M, Levin JZ, Thompson DA, Amit I, Adiconis X, Fan
525 L, Raychowdhury R, Zeng Q *et al*: **Full-length transcriptome assembly from RNA-**
526 **Seq data without a reference genome**. *Nat Biotechnol* 2011, **29**(7):644-652.
527 15. Papastamoulis P, Hensman J, Glaus P, Rattray M: **Improved variational Bayes**
528 **inference for transcript expression estimation**. *Stat Appl Genet Mol Biol* 2014,
529 **13**(2):203-216.
530 16. Bray NL, Pimentel H, Melsted P, Pachter L: **Near-optimal probabilistic RNA-seq**
531 **quantification**. *Nat Biotechnol* 2016, **34**(5):525-527.
532 17. Li B, Dewey CN: **RSEM: accurate transcript quantification from RNA-Seq data**
533 **with or without a reference genome**. *BMC Bioinformatics* 2011, **12**:323.
534 18. Patro R, Duggal G, Love MI, Irizarry RA, Kingsford C: **Salmon provides fast and**
535 **bias-aware quantification of transcript expression**. *Nat Methods* 2017, **14**(4):417-
536 419.
537 19. Smith-Unna R, Boursnell C, Patro R, Hibberd JM, Kelly S: **TransRate: reference-free**
538 **quality assessment of de novo transcriptome assemblies**. *Genome Res* 2016,
539 **26**(8):1134-1144.
540 20. Zhao QY, Wang Y, Kong YM, Luo D, Li X, Hao P: **Optimizing de novo transcriptome**
541 **assembly from short-read RNA-Seq data: a comparative study**. *BMC*
542 *Bioinformatics* 2011, **12 Suppl 14**:S2.
543 21. Li B, Fillmore N, Bai Y, Collins M, Thomson JA, Stewart R, Dewey CN: **Evaluation**
544 **of de novo transcriptome assemblies from RNA-Seq data**. *Genome Biol* 2014,
545 **15**(12):553.
546 22. Kanitz A, Gypas F, Gruber AJ, Gruber AR, Martin G, Zavolan M: **Comparative**
547 **assessment of methods for the computational inference of transcript isoform**
548 **abundance from RNA-seq data**. *Genome Biol* 2015, **16**:150.
549 23. Zhang C, Zhang B, Lin LL, Zhao S: **Evaluation and comparison of computational**
550 **tools for RNA-seq isoform quantification**. *BMC Genomics* 2017, **18**(1):583.
551 24. Wang S, Gribskov M: **Comprehensive evaluation of de novo transcriptome**
552 **assembly programs and their effects on differential gene expression analysis**.
553 *Bioinformatics* 2017, **33**(3):327-333.
554 25. Altschul SF, Madden TL, Schaffer AA, Zhang J, Zhang Z, Miller W, Lipman DJ:

555 **Gapped BLAST and PSI-BLAST: a new generation of protein database search**
556 **programs**. *Nucleic Acids Res* 1997, **25**(17):3389-3402.
557 26. Nookaew I, Papini M, Pornputtapong N, Scalcinati G, Fagerberg L, Uhlen M, Nielsen
558 J: **A comprehensive comparison of RNA-Seq-based transcriptome analysis from**
559 **reads to differential gene expression and cross-comparison with microarrays: a**
560 **case study in Saccharomyces cerevisiae**. *Nucleic Acids Res* 2012, **40**(20):10084-
561 10097.
562 27. Liu D, Xiong H, Ellis AE, Northrup NC, Rodriguez CO, Jr., O'Regan RM, Dalton S,
563 Zhao S: **Molecular homology and difference between spontaneous canine**
564 **mammary cancer and human breast cancer**. *Cancer Res* 2014, **74**(18):5045-5056.
565 28. Griebel T, Zacher B, Ribeca P, Raineri E, Lacroix V, Guigo R, Sammeth M: **Modelling**
566 **and simulating generic RNA-Seq experiments with the flux simulator**. *Nucleic*
567 *Acids Res* 2012, **40**(20):10073-10083.
568 29. Aken BL, Achuthan P, Akanni W, Amode MR, Bernsdorff F, Bhai J, Billis K, Carvalho-
569 Silva D, Cummins C, Clapham P *et al*: **Ensembl 2017**. *Nucleic Acids Res* 2017,
570 **45**(D1):D635-D642.
571 30. Andrews S: **FastQC: A quality control tool for high throughput sequence data**.
572 *Reference Source* 2010.
573 31. Bolger AM, Lohse M, Usadel B: **Trimmomatic: a flexible trimmer for Illumina**
574 **sequence data**. *Bioinformatics* 2014, **30**(15):2114-2120.
575 32. Li H, Durbin R: **Fast and accurate short read alignment with Burrows-Wheeler**
576 **transform**. *Bioinformatics* 2009, **25**(14):1754-1760.
577 33. Li B, Ruotti V, Stewart RM, Thomson JA, Dewey CN: **RNA-Seq gene expression**
578 **estimation with read mapping uncertainty**. *Bioinformatics* 2010, **26**(4):493-500.
579 34. Pachter L: **Models for transcript quantification from RNA-Seq**. *arXiv preprint*
580 *arXiv:11043889* 2011.
581 35. Simpson JT, Wong K, Jackman SD, Schein JE, Jones SJ, Birol I: **ABySS: a parallel**
582 **assembler for short read sequence data**. *Genome Res* 2009, **19**(6):1117-1123.
583 36. Langmead B, Salzberg SL: **Fast gapped-read alignment with Bowtie 2**. *Nat Methods*
584 2012, **9**(4):357-359.
585 37. Soneson C, Love MI, Robinson MD: **Differential analyses for RNA-seq: transcript-**
586 **level estimates improve gene-level inferences**. *F1000Res* 2015, **4**:1521.
587 38. Wang L, Si Y, Dedow LK, Shao Y, Liu P, Brutnell TP: **A low-cost library construction**
588 **protocol and data analysis pipeline for Illumina-based strand-specific multiplex**

589 **RNA-seq**. *PLoS One* 2011, **6**(10):e26426.
590 39. Roberts A, Trapnell C, Donaghey J, Rinn JL, Pachter L: **Improving RNA-Seq**
591 **expression estimates by correcting for fragment bias**. *Genome Biol* 2011, **12**(3):R22.
592 40. Marinov GK, Williams BA, McCue K, Schroth GP, Gertz J, Myers RM, Wold BJ: **From**
593 **single-cell to cell-pool transcriptomes: stochasticity in gene expression and RNA**
594 **splicing**. *Genome Res* 2014, **24**(3):496-510.
595 41. Rhoads A, Au KF: **PacBio Sequencing and Its Applications**. *Genomics Proteomics*
596 *Bioinformatics* 2015, **13**(5):278-289.

597

Figure Legends

Fig. 1: Construction of Ambiguity Network. The diagram illustrates pairwise alignments in a contig set and how the ambiguity network was constructed. The connected component was first initialized given the contig sequences, creating a single cluster for each sequence. By analyzing the global alignment between contigs (the blue dot lines), the cluster expanded by union two contig cluster at a time if the alignment length between the sequence is over 90% of the length for either sequence. Note that the ambiguity network was constructed for both contig and transcript set. For the purpose of simplicity, we only illustrated the scenario for contigs in this figure.

Fig. 2: Examples of Contig Categories. The diagram gives examples for each contig category we analyzed throughout this study. The middle column shows an example for each category, while the right column portrays the relation of contigs and transcripts in network representation. The sequence nodes are connected together in solid line if they are in the same ambiguity cluster. On the other hand, the blue dot arrow represents the transcript assignment for the contigs. The analysis of contigs labeled as full-length, incompleteness and over-extended exclude the factor of sequence ambiguity. On the contrary, family-collapse and duplication remove the potential effect of assembly completeness, focusing only on the impact of redundant or duplicated sequences.

Fig. 3: Quantification Error for Unique Sequences. The box plots illustrate the relative quantification error for unique contigs for simulated dataset. The estimation of contig abundance is made by Kallisto based on Trinity assembly. The contigs are separated by the extent of assembly completeness, the numbers on the X-axis represents the lower bound of difference in length. For instance, the contigs locate on -10 means that the percentage of difference in length is in the range of $[-10, 0)$. The data is color coded based on the contig categories. The box plots suggest that the estimation made on full-length contigs yield the smallest relative error, while the incomplete contigs show over-estimation and over-extended contigs show under-estimation on quantification

Fig. 4: Scatter plots of Estimated Abundance and Ground Truth Expression for Unique Sequences. The scatter plots illustrate the estimated and ground truth abundance for contigs categorized as full-length, incompleteness and over-extension of simulated dog dataset. The

estimation of contig abundance is made by Kallisto based on Trinity assembly. The metrics are recorded in $log_2(TPM + 1)$. The data points are color coded based on the relative quantification error, with blue represents under-estimation and orange for over-estimation. In general, the estimation on expression for full-length contigs is highly reliable. There are some incomplete contigs with over-estimated abundance. Moreover, the correlation coefficients for the estimation of incomplete contigs are also relatively lower than that of full-length contigs. As for over-extended contigs, a marginal under-estimation in quantification can be observed.

Fig. 5. Correlation Coefficients between Estimated Abundance and Ground Truth Expression for Unique Sequences. The figures illustrate the Pearson's and Spearman's correlation coefficients between estimated abundance and ground truth expression. In general, the estimation based on full-length contigs have considerably high correlation with the ground truth expression of corresponding transcripts. In contrast, the incomplete and over-extended contigs show relatively lower correlation coefficients. There are significantly low correlation coefficients in the rnaSPAdes assembly based on simulated yeast data; however, due to a small number of data (n = 11), it should not be used to draw conclusion on this dataset.

Fig. 6: Scatter plots of Estimated Abundance and Ground Truth Expression for Family-Collapse Sequences. The scatter plots illustrate the estimated and ground truth abundance for contigs categorized as family-collapse of simulated dog dataset. The estimation of contig abundance is made by Kallisto based on Trinity assembly. The metrics are recorded in $log_2(TPM + 1)$. The data points are color coded based on the relative quantification error, with blue represents under-estimation and orange for over-estimation. Since there are more than one transcripts correspond to one contig, we categorize the expression of corresponding transcript into (1) transcript with the maximum alignment score, (2) transcript with the highest expression, and (3) others. In general, the estimated abundance of the contig actually reflect to the transcript with the highest expression.

Fig. 7: Box Plots for the Relative Error of Duplicated Contigs. The box plots illustrate the relative quantification error for duplicated contigs of experimental mouse dataset. The contigs are separated by the proportion of maximum estimated abundance in the connected component, the numbers on the X-axis represents the lower bound of the proportion. For instance, the contigs locate on 0.45 means that the percentage of difference in length is in the range of $[0.45, 0.50)$. Since there are more than one contigs which are assigned with the same transcripts.

We would like to find out which contigs' estimated abundance can accurately reflect the expression of the transcripts. Here, we categorize the quantification error into three categories: (1) based on the contigs with the highest alignment score, (2) based on the contigs that are allocated with the most RNA reads and (3) the total expression of connected component of the contigs. The box plots suggest that contigs with the highest alignment score or the highest estimation made within the connected component have considerably lower quantification error if most of the reads are assigned to one specific contig. However, when the quantifiers allocate the RNA reads evenly to the contigs within the connected component, it is advisable to use the total expression of connected component in order to get the accurate estimation upon the expression of transcripts.

Fig. 8: Scatter plots of Estimated Abundance and Ground Truth Expression for All Sequences. The scatter plots illustrate the estimated and ground truth abundance for all the contigs of simulated dog dataset. The estimation of contig abundance is made by Kallisto based on Trinity assembly. The metrics are recorded in $log_2(TPM + 1)$. The data points are color coded based on the relative quantification error, with blue represents under-estimation and orange for over-estimation. We looked through all the valid assignment of transcripts for each contig and we demonstrated four different methods: (1) selecting the transcripts with the highest alignment score for each contig, followed by selecting the contig with the highest alignment score for each transcript (ATAC), (2) selecting the transcripts with the highest alignment score for each contig, followed by selecting the contig with the highest RPEA score in the connected component (ATHC), (3) selecting the transcripts with the highest expression in the connected component, followed by selecting the contig with the highest alignment score for each transcript (HTAC), and (4) selecting the transcripts with the highest expression in the connected component, followed by selecting the contig with the highest RPEA score in the connected component (HTHC) We would like to understand whether the estimated abundance for both methods can be used to accurately estimate the expression of transcript. In general, the estimated abundance of the contig with the highest number of allocated reads in the connected component yield a more accurate estimation.

Additional Files

Additional File 1. Title: Supplementary Tables. Description of data: Table S1 to Table S6.

Additional File 2. Title: Supplementary Figures. Description of data: Fig. S1 to Fig S6.

sequences

contig a	TTACACAATCGTAGCATGTATG
contig b	TACACAATCGTAGCATGTATGG
contig c	AATCGTAG
contig d	CAATCGTAGCATGTATGG
contig e	GACCTTTGTTCACGTTTGCCCAT

alignments

```
contig a   TTACACAATCGTAGCATGTATG
           |||||||||||||||||||||
contig b   TACACAATCGTAGCATGTATGG
```

alignment length ≥ 90% length of both sequences

```
contig c   AATCGTAG
           ||||||||
contig d   CAATCGTAGCATGTATGG
```

alignment length ≥ 90% length of either sequence

```
contig a   TTACACAATCGTAGCATGTATG
               ||||||||
contig c       AATCGTAG
```

alignment length ≥ 90% length of either sequence

network initialization

network operation

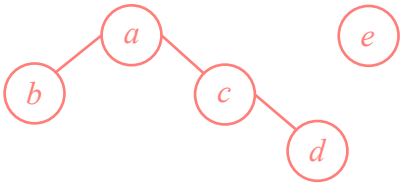

union(a, c) *union*(a, b) *union*(c, d)

Full-length	*contig* *transcript*	TTACACAATCGTAG TACACAATCGTAGC	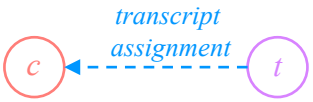
Incompleteness	*contig* *transcript*	TACA TACACAATCGTAGC	
Over-extended	*contig* *transcript*	TTACACAATCGTAG CACA	
Family-collapse	*contig* *transcript a* *transcript b* *transcript c*	TTACACAATCGTAG TACACAATCGTAGC TTACACGATCGTA CTACACAATGGTAG	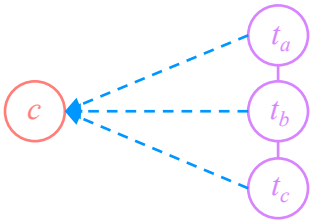
Duplication	*contig a* *contig b* *contig c* *transcript*	TTACACAATCGTAG TACACAATCGTAGC TTACACGATCGTA CTACACAATGGTAG	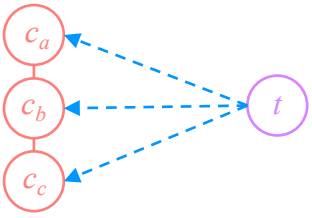

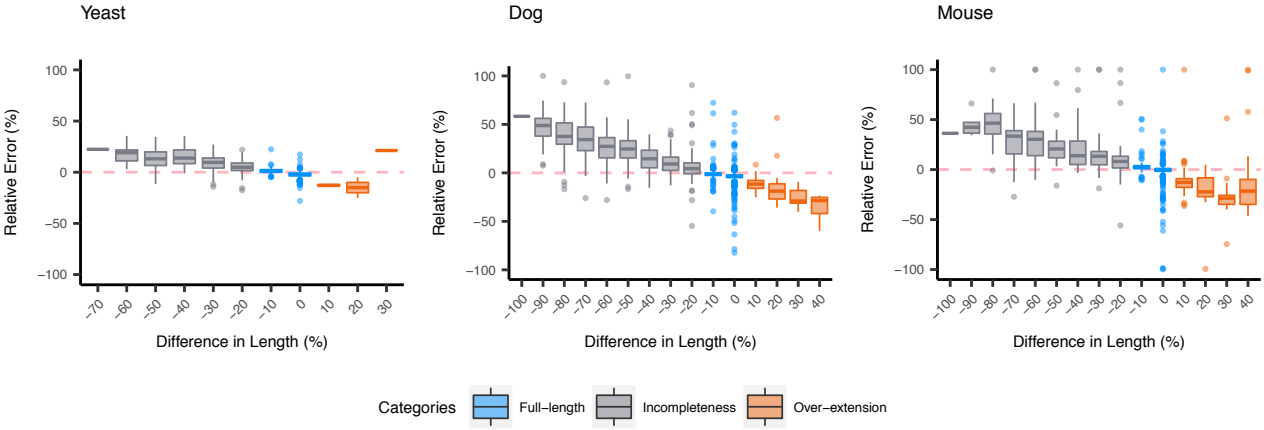
Yeast
Dog
Mouse
Relative Error (%)
Difference in Length (%)
Categories
Full−length
Incompleteness
Over−extension

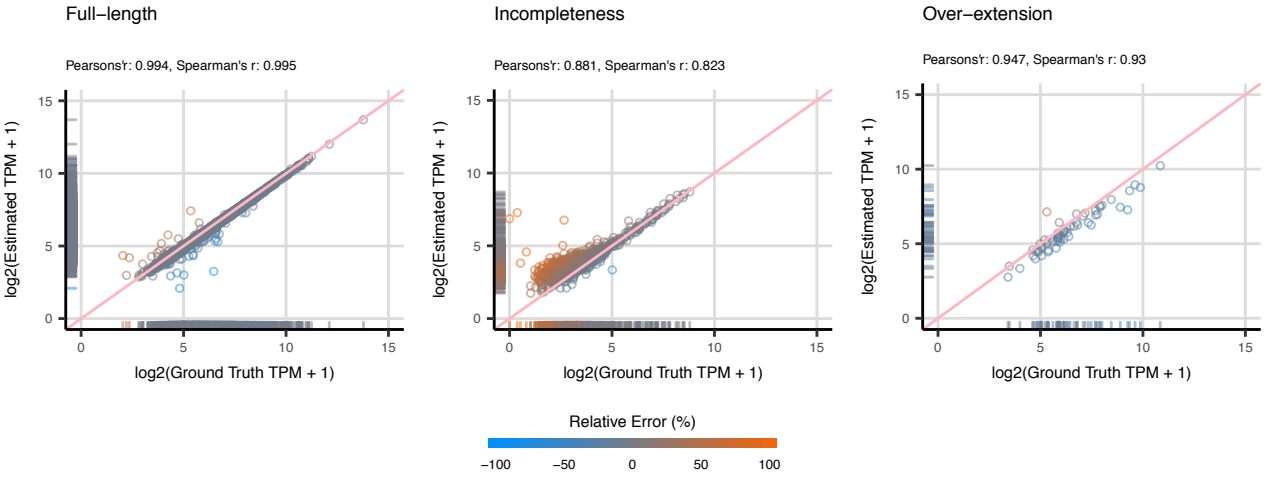
Full−length
Pearsons'r: 0.994, Spearman's r: 0.995
Incompleteness
Pearsons'r: 0.881, Spearman's r: 0.823
Over−extension
Pearsons'r: 0.947, Spearman's r: 0.93
log2(Estimated TPM + 1)
log2(Ground Truth TPM + 1)
0
5
10
15
Relative Error (%)
−100
−50
0
50
100

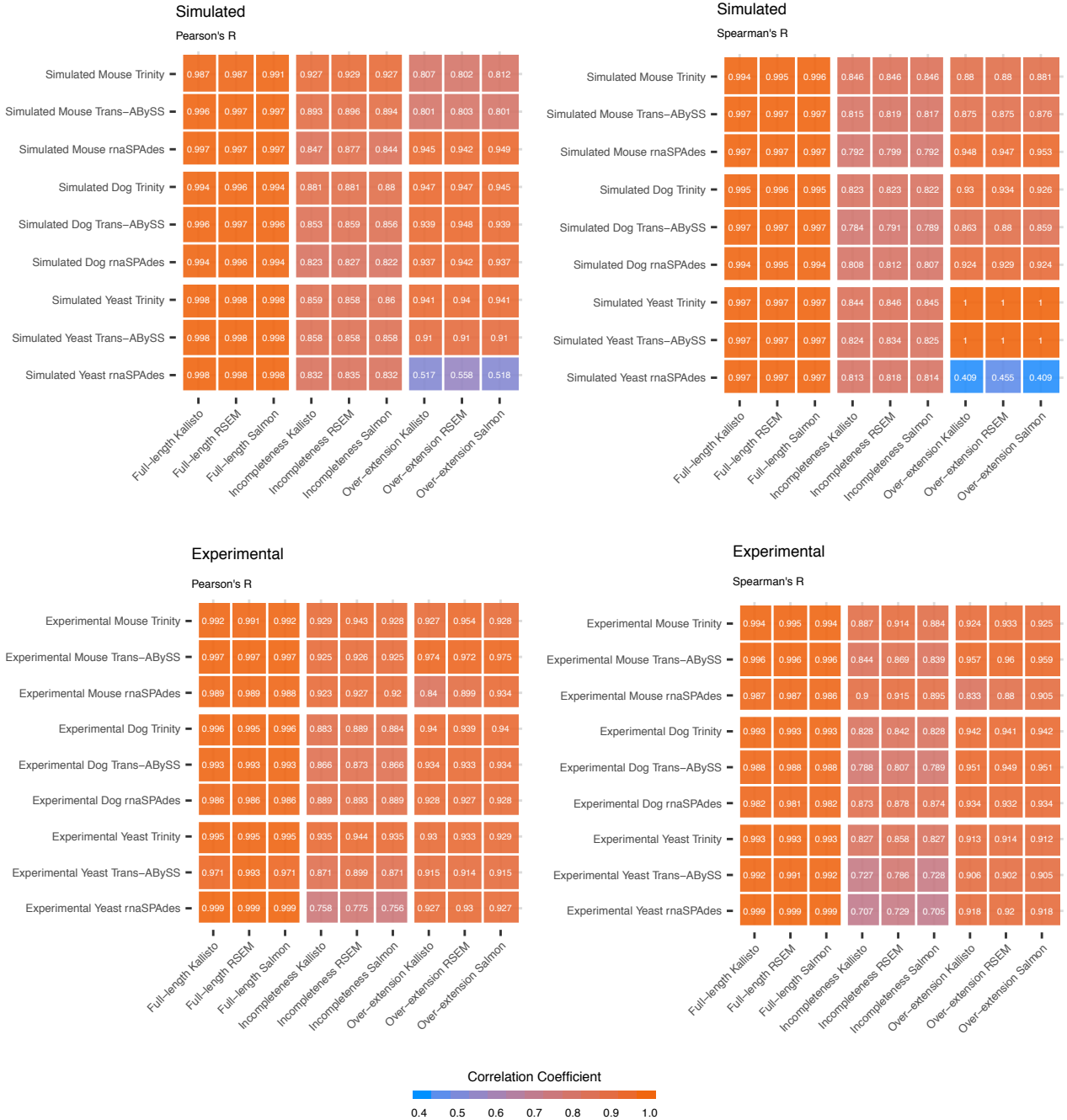
Simulated
Pearson's R
Simulated Mouse Trinity 0.987 0.987 0.991 0.927 0.929 0.927 0.807 0.802 0.812
Simulated Mouse Trans−ABySS 0.996 0.997 0.997 0.893 0.896 0.894 0.801 0.803 0.801
Simulated Mouse rnaSPAdes 0.997 0.997 0.997 0.847 0.877 0.844 0.945 0.942 0.949
Simulated Dog Trinity 0.994 0.996 0.994 0.881 0.881 0.88 0.947 0.947 0.945
Simulated Dog Trans−ABySS 0.996 0.997 0.996 0.853 0.859 0.856 0.939 0.948 0.939
Simulated Dog rnaSPAdes 0.994 0.996 0.994 0.823 0.827 0.822 0.937 0.942 0.937
Simulated Yeast Trinity 0.998 0.998 0.998 0.859 0.858 0.86 0.941 0.94 0.941
Simulated Yeast Trans−ABySS 0.998 0.998 0.998 0.858 0.858 0.858 0.91 0.91 0.91
Simulated Yeast rnaSPAdes 0.998 0.998 0.998 0.832 0.835 0.832 0.517 0.558 0.518
Full−length Kallisto
Full−length RSEM
Full−length Salmon
Incompleteness Kallisto
Incompleteness RSEM
Incompleteness Salmon
Over−extension Kallisto
Over−extension RSEM
Over−extension Salmon
Simulated
Spearman's R
Simulated Mouse Trinity 0.994 0.995 0.996 0.846 0.846 0.846 0.88 0.88 0.881
Simulated Mouse Trans−ABySS 0.997 0.997 0.997 0.815 0.819 0.817 0.875 0.875 0.876
Simulated Mouse rnaSPAdes 0.997 0.997 0.997 0.792 0.799 0.792 0.948 0.947 0.953
Simulated Dog Trinity 0.995 0.996 0.995 0.823 0.823 0.822 0.93 0.934 0.926
Simulated Dog Trans−ABySS 0.997 0.997 0.997 0.784 0.791 0.789 0.863 0.88 0.859
Simulated Dog rnaSPAdes 0.994 0.995 0.994 0.808 0.812 0.807 0.924 0.929 0.924
Simulated Yeast Trinity 0.997 0.997 0.997 0.844 0.846 0.845 1 1 1
Simulated Yeast Trans−ABySS 0.997 0.997 0.997 0.824 0.834 0.825 1 1 1
Simulated Yeast rnaSPAdes 0.997 0.997 0.997 0.813 0.818 0.814 0.409 0.455 0.409
Full−length Kallisto
Full−length RSEM
Full−length Salmon
Incompleteness Kallisto
Incompleteness RSEM
Incompleteness Salmon
Over−extension Kallisto
Over−extension RSEM
Over−extension Salmon
Experimental
Pearson's R
Experimental Mouse Trinity 0.992 0.991 0.992 0.929 0.943 0.928 0.927 0.954 0.928
Experimental Mouse Trans−ABySS 0.997 0.997 0.997 0.925 0.926 0.925 0.974 0.972 0.975
Experimental Mouse rnaSPAdes 0.989 0.989 0.988 0.923 0.927 0.92 0.84 0.899 0.934
Experimental Dog Trinity 0.996 0.995 0.996 0.883 0.889 0.884 0.94 0.939 0.94
Experimental Dog Trans−ABySS 0.993 0.993 0.993 0.866 0.873 0.866 0.934 0.933 0.934
Experimental Dog rnaSPAdes 0.986 0.986 0.986 0.889 0.893 0.889 0.928 0.927 0.928
Experimental Yeast Trinity 0.995 0.995 0.995 0.935 0.944 0.935 0.93 0.933 0.929
Experimental Yeast Trans−ABySS 0.971 0.993 0.971 0.871 0.899 0.871 0.915 0.914 0.915
Experimental Yeast rnaSPAdes 0.999 0.999 0.999 0.758 0.775 0.756 0.927 0.93 0.927
Full−length Kallisto
Full−length RSEM
Full−length Salmon
Incompleteness Kallisto
Incompleteness RSEM
Incompleteness Salmon
Over−extension Kallisto
Over−extension RSEM
Over−extension Salmon
Experimental
Spearman's R
Experimental Mouse Trinity 0.994 0.995 0.994 0.887 0.914 0.884 0.924 0.933 0.925
Experimental Mouse Trans−ABySS 0.996 0.996 0.996 0.844 0.869 0.839 0.957 0.96 0.959
Experimental Mouse rnaSPAdes 0.987 0.987 0.986 0.9 0.915 0.895 0.833 0.88 0.905
Experimental Dog Trinity 0.993 0.993 0.993 0.828 0.842 0.828 0.942 0.941 0.942
Experimental Dog Trans−ABySS 0.988 0.988 0.988 0.788 0.807 0.789 0.951 0.949 0.951
Experimental Dog rnaSPAdes 0.982 0.981 0.982 0.873 0.878 0.874 0.934 0.932 0.934
Experimental Yeast Trinity 0.993 0.993 0.993 0.827 0.858 0.827 0.913 0.914 0.912
Experimental Yeast Trans−ABySS 0.992 0.991 0.992 0.727 0.786 0.728 0.906 0.902 0.905
Experimental Yeast rnaSPAdes 0.999 0.999 0.999 0.707 0.729 0.705 0.918 0.92 0.918
Full−length Kallisto
Full−length RSEM
Full−length Salmon
Incompleteness Kallisto
Incompleteness RSEM
Incompleteness Salmon
Over−extension Kallisto
Over−extension RSEM
Over−extension Salmon
Correlation Coefficient
0.4 0.5 0.6 0.7 0.8 0.9 1.0

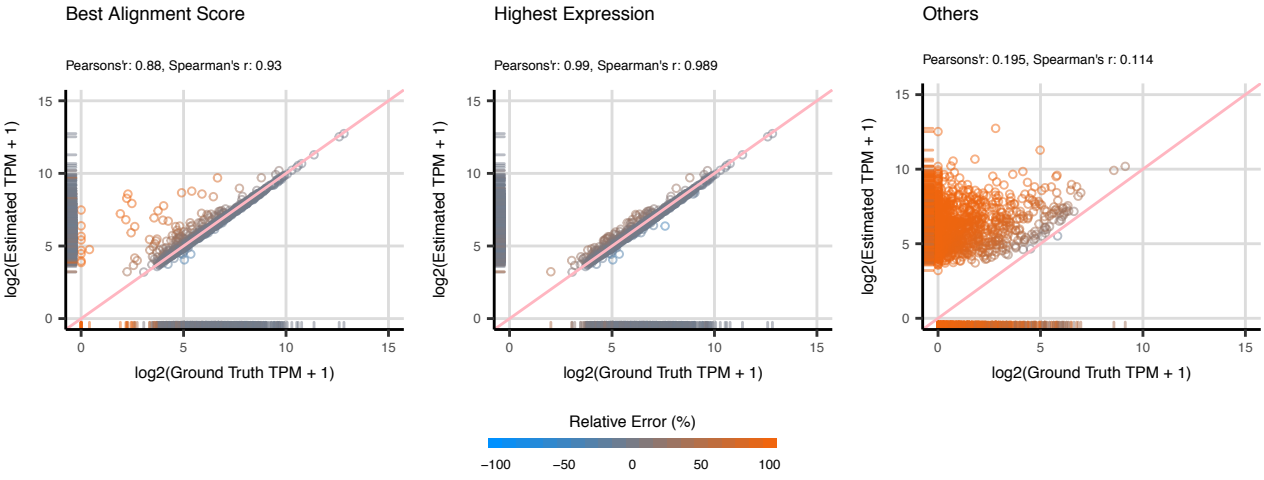
Best Alignment Score
Pearsons'r: 0.88, Spearman's r: 0.93
Highest Expression
Pearsons'r: 0.99, Spearman's r: 0.989
Others
Pearsons'r: 0.195, Spearman's r: 0.114
log2(Estimated TPM + 1)
log2(Ground Truth TPM + 1)
0
5
10
15
Relative Error (%)
−100
−50
0
50
100

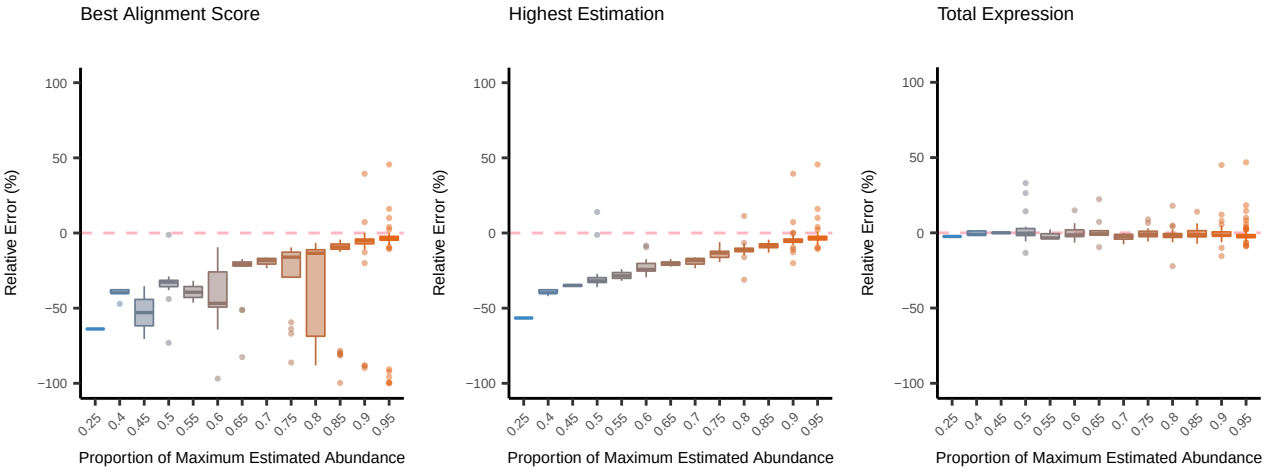
Best Alignment Score
Highest Estimation
Total Expression
Relative Error (%)
100
50
0
−50
−100
0.25
0.4
0.45
0.5
0.55
0.6
0.65
0.7
0.75
0.8
0.85
0.9
0.95
Proportion of Maximum Estimated Abundance

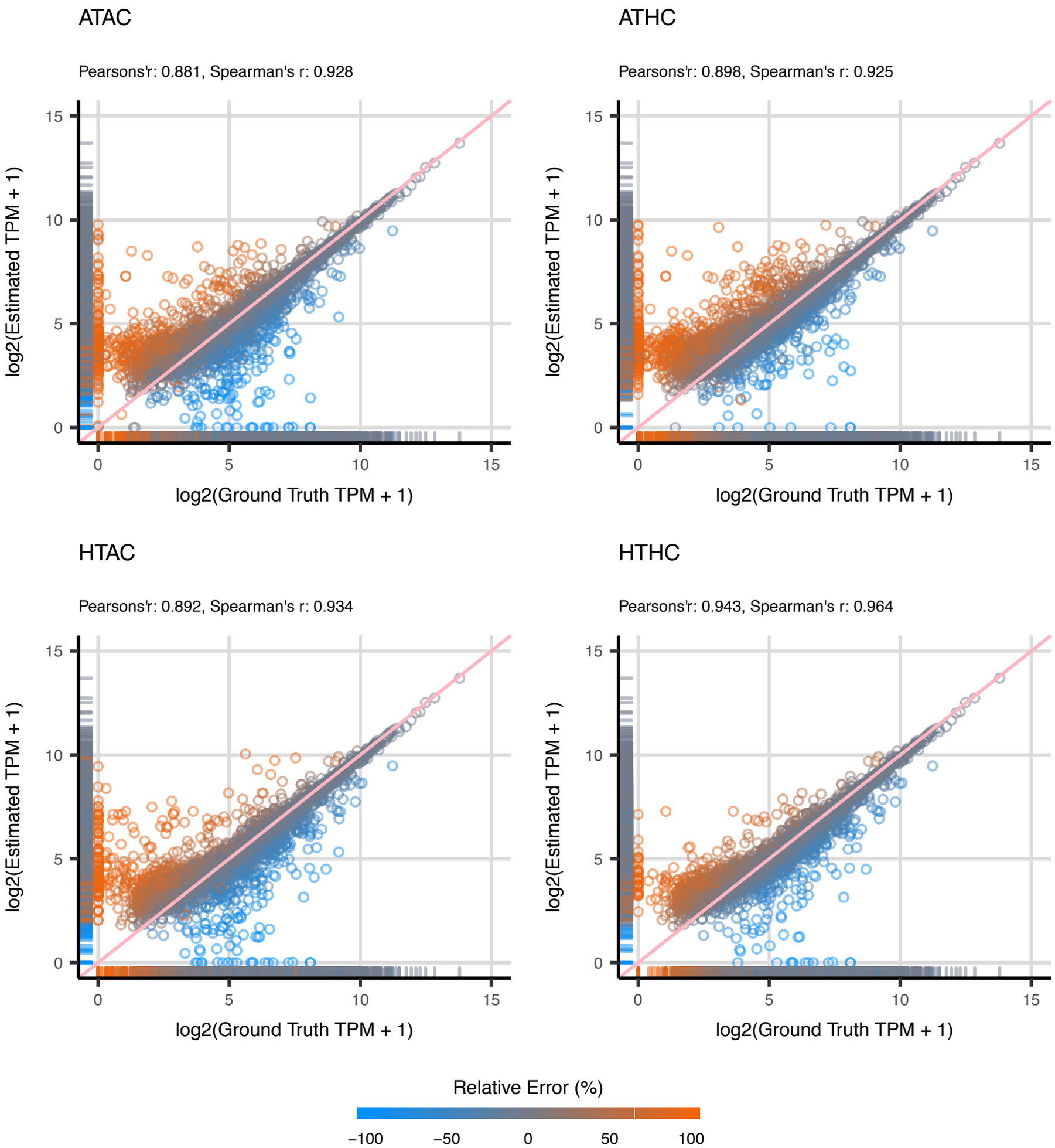
ATAC
Pearsons'r: 0.881, Spearman's r: 0.928
ATHC
Pearsons'r: 0.898, Spearman's r: 0.925
HTAC
Pearsons'r: 0.892, Spearman's r: 0.934
HTHC
Pearsons'r: 0.943, Spearman's r: 0.964
log2(Estimated TPM + 1)
log2(Ground Truth TPM + 1)
0
5
10
15
Relative Error (%)
−100
−50
0
50
100